

Formation of High Mass X-ray Black Hole Binaries

G.E. Brown^{a,1} A. Heger^{b,2} N. Langer^{c,3} C.-H. Lee^{a,d,4}
 S. Wellstein^{e,5} H.A. Bethe^f

^a*Department of Physics & Astronomy, State University of New York,
 Stony Brook, New York 11794, USA*

^b*Department of Astronomy and Astrophysics, University of California,
 Santa Cruz, CA 95064, USA*

^c*Astronomical Institute, P.O. Box 80000, NL-3508 TA Utrecht, The Netherlands*

^d*School of Physics, Korea Institute for Advanced Study, Seoul 130-012, Korea*

^e*Institut für Physik, Universität Potsdam, Am Neuen Palais 10,
 D-14415 Potsdam, Germany*

^f*Floyd R. Newman Laboratory of Nuclear Studies, Cornell University,
 Ithaca, New York 14853, USA*

Abstract

The discrepancy in the past years of many more black-hole soft X-ray transients (SXTs), of which a dozen have now been identified, had challenged accepted wisdom in black hole evolution. Reconstruction in the literature of high-mass X-ray binaries has required stars of up to $\sim 40 M_{\odot}$ to evolve into low-mass compact objects, setting this mass as the limit often used for black hole formation in population syntheses. On the other hand, the sheer number of inferred SXTs requires that many, if not most, stars of ZAMS masses $20 - 35 M_{\odot}$ end up as black holes (Portegies Zwart et al. 1997; Ergma & van den Heuvel 1998).

In this paper we show that this can be understood by challenging the accepted wisdom that the result of helium core burning in a massive star is independent of whether the core is covered by a hydrogen envelope, or “naked” while it burns. The latter case occurs in binaries when the envelope of the more massive star is transferred to the companion by Roche Lobe overflow while in either main sequence or red giant stage. For solar metallicity, whereas the helium cores which burn while naked essentially never go into high-mass black holes, those that burn while clothed do so, beginning at ZAMS mass $\sim 20 M_{\odot}$, the precise mass depending on the $^{12}\text{C}(\alpha, \gamma)^{16}\text{O}$ rate as we outline. In this way the SXTs can be evolved, provided that the H envelope of the massive star is removed only following the He core burning.

Whereas this scenario was already outlined in 1998 by Brown, Lee, & Bethe (1999) their work was based on evolutionary calculations of Woosley, Langer, & Weaver (1995) which employed wind loss rates which were too high. In this article we collect

results for lower, more correct wind loss rates, finding that these change the results only little.

We go into the details of carbon burning in order to reconstruct why the low Fe core masses from naked He stars are relatively insensitive to wind loss rate. The main reason is that without the helium produced by burning the hydrogen envelope, which is convected to the carbon in a clothed star, a central ^{12}C abundance of $\sim 1/3$ remains unburned in a naked star following He core burning. The later convective burning through $^{12}\text{C}+^{12}\text{C}$ reactions occurs at a temperature $T \sim 80$ keV.

Finally, we show that in order to evolve a black hole of mass $\gtrsim 10 M_\odot$ such as observed in Cyg X-1, even employing extremely massive progenitors of ZAMS mass $\gtrsim 60 M_\odot$ for the black hole, the core must be covered by hydrogen during a substantial fraction of the core burning. In other words, the progenitor must be a WNL star. We evolve Cyg X-1 in an analogous way to which the SXTs are evolved, the difference being that the companion in Cyg X-1 is more massive than those in the SXTs, so that Cyg X-1 shines continuously.

Key words: binaries: close – stars: neutron – black hole physics – stars: evolution – stars: Wolf-Rayet – stars: mass-loss

¹ E-mail: popenoe@nuclear.physics.sunysb.edu

² E-mail: alex@ucolick.org

³ E-mail: N.Langer@astro.uu.nl

⁴ E-mail: chlee@kias.re.kr

⁵ E-mail: stephan@astro.physik.uni-potsdam.de

1 Introduction

Accepted wisdom in the astrophysical community (for recent relevant articles see Portegies Zwart, Verbunt, & Ergma 1997; Ergma & van den Heuvel 1998) has been that the results of burning the helium core of a star are independent of whether it is covered by a hydrogen envelope or whether it burns as a “naked” star, the envelope having been removed; e.g. by Roche Lobe overflow in main sequence or red giant stage of the star. This latter situation takes place in binary evolution where the evolution referred to in the above two articles determines the black hole progenitors to have ZAMS mass $> 40 M_{\odot}$. Thus, this mass limit for black hole formation is adopted for the evolution of the black hole soft X-ray transients (SXTs) in these articles. On the other hand, as acknowledged in them, the observed number of SXTs requires that many, if not most, stars of ZAMS masses in the interval of $\sim 20 - 35 M_{\odot}$ evolve into high-mass black holes, of mass $\gtrsim 6 M_{\odot}$.

Brown, Lee, & Bethe (1999) offered as explanation of the large number of SXTs that stars in the mass range $\sim 20 - 35 M_{\odot}$ could evolve into high-mass black holes as long as their H envelope was lifted off by the companion star only after the He core burning was complete (Case C mass transfer). If it were lifted off earlier, too small an Fe core evolved to make a high-mass black hole. In fact, Timmes, Woosley, & Weaver (1996) had found that Fe cores of Type Ib supernovae were systematically of lower mass than those of Type II, basically the same concept. The Brown, Lee, & Bethe scenario had been outlined by Brown, Weingartner, & Wijers (1996). Their results were not generally believed, however, because the calculation of Woosley, Langer, & Weaver (1995) on which they relied employed mass loss rates that were too large by a factor of 2 to 3 for the naked He stars. Thus, the present work using lower, more correct, rates is necessary.

Wellstein & Langer (2000) recalculated the evolution of naked He cores to their carbon-oxygen cores with wind loss rates lowered by a factor of 2, and in some cases by larger factors, finding that because of feedbacks, the total wind loss scaled more slowly than linearly with the multiplier on the wind loss rate. In work that we describe here, Alexander Heger, using the Woosley & Weaver computer program Kepler, evolved the CO cores further to their Fe cores. These are not sufficiently massive to end up as high-mass black holes; in fact, the situation is nearly the same as found by Brown, Weingartner & Wijers (1996) where too large He star mass loss rates had been used. Our main objective in this article is to explain why the masses of the final Fe cores depend only insensitively on the He core mass loss rates. We interpret the Fe core mass as a good indicator of the final compact core mass because binding energy corrections and mass fallback very nearly compensate each other (Brown, Weingartner, & Wijers 1996).

The plan of this paper is as follows:

In Sec. 2 we discuss the improved measurements of wind losses as deduced from Wolf-Rayet stars.

In Sec. 3 we show that the large differences between “naked” and “clothed” He star burning can be understood in terms of the different ways in which carbon burns in the two cases.

In Sec. 4 we deal with a possible evolution of the $\sim 10 M_\odot$ black hole in Cyg X-1, suggesting that there may be an analogy with the evolution of transient sources; namely that the He core must be kept covered by H during most of its burning. This requires a very massive progenitor, a WNL star.

In Sec. 5 we give simple concluding remarks.

2 Wind Loss Rates in WNE’s (naked He stars)

It is the mass loss rate proposed by Langer (1989a) for hydrogen-free Wolf-Rayet stars, which replaced the previously used assumption of a constant Wolf-Rayet mass loss rate in many evolutionary calculations (Schaller et al. 1992; cf. WLW 1995), which leads to the small final masses of stars above $\sim 35 M_\odot$. This semi-empirical rate has been criticised as too high, one argument being the existence of massive black hole binaries. Indeed, recent studies of Wolf-Rayet stars show that originally measured wind losses have to be corrected downwards by a factor of 2...3 to account for their “clumpiness” (Hamann & Koesterke 1998). This is supported by polarisation measurements of the Thomson scattering, which depend linearly on the wind density (St.-Louis et al. 1993, Moffat & Robert 1994), and is in approximate agreement with the rates that would be deduced from the observed rate of increase in orbital periods for spherical mass loss

$$\frac{\dot{M}}{M} = \frac{\dot{P}}{2P} \quad (1)$$

in Wolf-Rayet binaries. In V444 Cygni $\dot{P} = 0.202 \pm 0.018 \text{ s yr}^{-1}$ was obtained by Khaliullin et al. (1984) and $M_{WR} = 9.3 \pm 0.5 M_\odot$ by Marchenko et al. (1994), resulting in

$$\dot{M}_{dyn} \simeq 1 \times 10^{-5} M_\odot \text{ yr}^{-1}. \quad (2)$$

This is to be compared with the

$$\dot{M} = 0.75 \times 10^{-5} M_{\odot} \text{ yr}^{-1} \quad (3)$$

obtained by St.-Louis et al. (1993) from the polarisation measurements. In later work Moffat & Robert (1994) arrive at a mean of $(0.7 \pm 0.1) \times 10^{-5} M_{\odot} \text{ yr}^{-1}$. For WNE (defined here as a Wolf-Rayet phase with vanishing surface hydrogen abundance) stars, WLW (1993) used a He wind rate of

$$\dot{M} = 5 \times 10^{-8} (M_{WR}/M_{\odot})^{2.6} \dot{M}_{\odot} \text{ yr}^{-1} \quad (4)$$

which would give a mass loss rate of $1.6 \times 10^{-5} M_{\odot} \text{ yr}^{-1}$ for a $9.3 M_{\odot}$ WR, a factor of 1.6 to 2.1 greater than eqs. (2) and (3). Given the errors in measurement, we feel safe in saying that the true wind loss rate is not less than 1/3 to 1/2 the WLW value. Furthermore, we should mention that absolute value slope of the mass loss relation Eq. (4) agrees well with the latest empirical mass loss rate determinations of Nugis & Lamers (2000).

However, decreasing the rate to 1/3 does not change our conclusions, as shown by recent calculations with such a reduced mass loss rates by Wellstein & Langer (1999), by Fryer et al. (2001), and by the calculations of Heger described later in this paper. These show that stars with initial masses below $60 M_{\odot}$ are unlikely to produce black holes more massive than $10 M_{\odot}$, from naked helium stars, although high mass black holes ($\sim 5 - 10 M_{\odot}$) may result from the ZAMS mass range $\sim 20 - 35 M_{\odot}$ employed by Brown, Lee, & Bethe (1999) provided Case C mass transfer occurs in the binary. The relative insensitivity of the final Fe core masses to the wind-loss rate depends somewhat intricately on the way carbon burns in a naked He core, as we describe in the next section.

Before we go on to the next section we discuss, however, the possible evolution of Cyg X-1, a continuously shining black hole binary where the black hole mass is observed to be $\gtrsim 10 M_{\odot}$. Even though massive stars are so prone to lose their hydrogen envelopes and then suffer extreme wind mass loss as hydrogen-free Wolf-Rayet stars, Langer (1987) pointed out that the most massive stars may in fact avoid this kind of evolution. The reason for doing so is that these stars, upon core hydrogen exhaustion, produce an extended region of intermediate hydrogen abundance in between the helium core and the hydrogen-rich envelope. While the latter is supposed to be lost quickly in a so called Luminous Blue Variable (LBV) stage (e.g., Stothers 2000), this intermediate region may be sufficiently massive that the star does not manage to blow it away during the ensuing so called WNL stage (defined here as a Wolf-Rayet phase with non-vanishing surface hydrogen abundance).

An example for the resulting evolutionary sequence O star \rightarrow LBV \rightarrow WNL \rightarrow SN is the $100 M_{\odot}$ sequence of Langer & El Eid (1986). Also WLW (1993) showed that the final masses of stars above $\sim 80 M_{\odot}$ may increase again for

larger initial masses, while stars in the range $\sim 35\ldots 60 M_{\odot}$ obey the opposite trend. Even using the high mass loss rate, their $85 M_{\odot}$ WRB star evolved a final He core of $9.71 M_{\odot}$. We will estimate in Section 4 that this can be brought up to $\sim 16 M_{\odot}$ with the lower, more correct, mass loss rates. The reason that the He core of the WLW $85 M_{\odot}$ star was so much more massive than that of their $60 M_{\odot}$ star, was not only the higher mass of the progenitor but the fact that the WNL stage of the $85 M_{\odot}$ comprised $\sim 40\%$ of the Wolf-Rayet stage, whereas that of the $60 M_{\odot}$ star was $\sim 25\%$. During the WNL stage the star is covered by hydrogen, so that the mass loss rate is smaller than it would have been for a naked He star, and moreover the helium core mass increases with time.

Although the evolution of star as massive as $\sim 85 M_{\odot}$ is very uncertain, we believe that the only possibility for them to end up in $\gtrsim 10 M_{\odot}$ black holes is an extended WNL stage, lasting a major fraction of the core helium burning. As we discuss below, these stars would have an active hydrogen burning shell source, whereas the existence of such a stage in a single massive star would probably not affect its evolution substantially, an expansion of the star due to hydrogen shell burning does give the possibility of common envelope evolution with a companion. In other words, the most massive stars are covered by H during much of their core He burning time, and this may enable them to end up as high-mass black holes.

3 “Naked” vs “Clothed” Helium Core Burning

3.1 *Central Carbon Abundances vs Convective Carbon Burning*

As noted earlier, Timmes et al. (1996) and Brown, Weingartner, & Wijers (1996) showed that compact cores which followed from “naked” helium stars were substantially less massive than followed from those “clothed” during helium burning with hydrogen envelopes. More recently, this has been explored in detail by Wellstein & Langer (1999) and Fryer et al. (2001). An important property of the stellar core that is significantly influenced by this difference is the carbon abundance in the core at central helium depletion. If its abundance is high enough, central carbon burning become exothermic enough to significantly overcome the neutrino losses and burn in a convective core. Otherwise the first convective burning of carbon can only appear in a shell source. The carbon abundance also has significant effect on the location, duration, and extent of the carbon burning shells. For example, as the carbon abundance goes to zero, no convective shell burning occurs either. The lower the carbon abundance, the further out the first shell forms. The location of the last carbon-burning shell sets the size of the carbon-free core which determines

the final evolution of the star and the sizes of the iron core (possible direct black hole formation) and the silicon core (possible black hole formation by fall-back).

There are two major factors that contribute to the resulting carbon abundance after core helium depletion. The first is the dependence on the mass of the helium core and results chiefly from the different behavior of the $^{12}\text{C}(\alpha, \gamma)^{16}\text{O}$ reaction, as described clearly by Weaver & Woosley (1993). Since this is important to our development, we repeat the argument, supplemented by more recent developments.

Carbon is formed in the triple α -process; since this is a three-body process, it depends on the density as ρ^2 . Carbon is removed, when possible, by the $^{12}\text{C}(\alpha, \gamma)^{16}\text{O}$ process, which goes linearly with ρ . Now, for massive helium cores the central density scales roughly as $M^{-1/6}$. With increasing helium core mass this implies that carbon formation, which goes as ρ^2 , will be cut down, compared with $^{12}\text{C}(\alpha, \gamma)^{16}\text{O}$, which goes as ρ . Here, we also note that both the $^{12}\text{C}(\alpha, \gamma)^{16}\text{O}$ reaction and the triple α -process have very similar temperature dependence in the temperature regime of central helium burning, $2 \times 10^8 \text{ K}$, i.e., the carbon production does not depend on temperature in this regime.

This means that there is a mass above which the post-helium burning central carbon abundance is low enough to skip central carbon burning. Woosley & Weaver (1995) found this transition at a mass of $19 M_\odot$. However, this limit strongly depends on the still uncertain $^{12}\text{C}(\alpha, \gamma)^{16}\text{O}$ reaction rate and the stellar evolution model, in particular the prescription used for convection or mixing processes in general, and also mass loss. On this last issue we elaborate later in more detail.

A bare helium star behaves differently from a clothed one in that its helium core does not grow in mass due to hydrogen shell burning, as is the case in clothed stars, but rather shrinks due to mass loss from the surface – the whole star is only a helium core, a Wolf-Rayet star. Generally, the convective core tends to comprise a larger fraction of the helium core, by mass, as the central helium abundance decreases, due to the density-dependence outlined above. This statement depends, again, somewhat on the description of semiconvection, but probably applies to most models with either Schwarzschild convection (e.g., Schaller et al. 1992), overshooting or fast semiconvection (e.g., Woosley & Weaver 1995), or rotationally induced mixing (Heger, Langer, Woosley 2000). Additionally, the mass fraction of the convective core also increases with the mass of helium core. However, bare helium cores (early-type Wolf-Rayet stars) experience mass loss rates that are sufficiently strong that the convective core actually tends to shrink in the run of its evolution, in particular also towards the end of helium burning, rather than grow, as it does in a clothed star. This is despite the fact that it still comprises an increasingly larger fraction of the

remaining total helium core. The important point is that a growth in mass of the convective core injects new helium into this convective core, while when the mass is constant or decreases, this injection does not occur.

As the triple alpha reaction depends on the third power of the helium mass fraction it loses against the $^{12}\text{C}(\alpha, \gamma)^{16}\text{O}$ reaction toward the end of central helium burning, i.e., carbon is mostly burned rather than produced toward the end of central helium burning. That switch typically appears at a central helium mass fraction of around 10–20%. Most importantly, as can be seen from the central carbon abundances at the end of He burning in Table 1, the He fraction is too low to burn the final carbon, which remains at a central abundance $\gtrsim 0.30$ for all mass stars. This is roughly double the carbon abundance necessary for convective carbon burning. It is seen in Table 2 that the central carbon abundance in naked He stars goes down only slowly with decreasing mass loss rate, although by the time the mass loss is reduced by a factor of 6 the convective burning stops. In the clothed stars the growth of the core and its accompanied injection of helium after this time thus leads to a further decrease of carbon as compared to the bare helium cores that do not have this additional supply of helium.

In Fig. 1 we show calculations carried out by Tom Weaver (priv. com. 1995) using the KEPLER code (Weaver, Zimmerman, & Woosley 1978; Woosley & Weaver 1995) on the central carbon abundance after core helium depletion for “clothed” (single) stars without (any) mass loss as function of ZAMS mass. The rapid drop in C_c at ZAMS mass $M_{\text{ZAMS}} \sim 20 M_{\odot}$ causes the disappearance of convective carbon burning.

3.2 Iron Core Masses

It is generally known that the central entropy rises with the mass of the star; so that the more entropy is carried off, the less massive will be the final Fe core. This statement can be made more quantitatively by using the Bethe, Brown, Applegate, & Lattimer (1979) conclusion that the entropy per nucleon in the Fe core is $\lesssim 1$, in units of the Boltzmann constant. For a ZAMS $20 M_{\odot}$, the central entropy in our Fe core is 0.76 per nucleon when the He core is burned clothed, 0.775 when burned naked; i.e., essentially the same. Thus, the total entropy of the Fe core is $\sim N_N$ considering some gradient towards higher entropy at the outer layers of the core, where N_N is the number of nucleons in it. In this way one can see directly that the entropy that is carried off during the evolution of the Fe core will diminish its mass.

In Fig. 2 we show iron core masses at the time of iron core collapse for a finely spaced grid of stellar masses (Heger, Woosley, Martinez-Pinedo, & Langanke

2001). Filled circles and crosses correspond to the core masses of “clothed” single stars. The circles were calculated by Tom Weaver (1995, priv. com.) using the same physics as in Woosley & Weaver (1995), whereas the crosses employ the improved weak rates by Langanke & Martinez-Píñedo (2000) for electron capture and beta decay. Although the latter are much smaller than the rates by Fuller, Fowler, & Newman (1985) used by Woosley & Weaver (1995), the final Fe core masses are not much changed, for reasons described by Heger, Woosley, Martinez-Pinedo, & Langanke (2001).

For “clothed” single stars, one sees an anticorrelation between the peak in Fe core masses at ZAMS mass $\sim 23 M_{\odot}$ and the minimum in C_c at ZAMS mass $\sim 21 M_{\odot}$. In other words, the peak around $23 M_{\odot}$ in ZAMS masses occurs just where the central carbon abundance at the end of helium core burning is at its minimum of $\sim 10\%$, too low for convective core burning or the formation of a carbon-burning convective shell close to the center of the star.

When sufficient carbon remains, it will be burned convectively in reactions such as $^{12}\text{C} + ^{12}\text{C} \rightarrow ^{24}\text{Mg}$, $^{20}\text{Ne} + \alpha$ etc., at a temperature of $70 - 80$ keV, several times higher than the ~ 20 keV needed for $^{12}\text{C}(\alpha, \gamma)^{16}\text{O}$. If the carbon abundance is lower, the carbon burning phases are reduced and typically bigger carbon-free cores result for otherwise similar stars. Therefore less energy is carried away by neutrinos and the entropy in the core stays higher. More massive silicon and iron cores can form in this case (Boyes, Heger, and Woosley 2001). This is clearly seen in Figures 1 & 2.

Although the central carbon abundance goes up again for ZAMS mass $\sim 25 M_{\odot}$, and the Fe core mass goes down, by such high masses the gravitational energy of the stellar envelope is large and it is difficult for the shock energy after collapse to blow it off, so we believe that these will go into high-mass black holes, as well as the stars of ZAMS mass $20 - 23 M_{\odot}$.

3.3 Formation of High-Mass Black Holes

Although there is a lot of uncertainty in the literature about the ZAMS masses which end up in high mass black holes, Bethe & Brown (1999) argued that this should occur at the proto compact core mass of

$$M_{PC} \sim 1.8 M_{\odot}. \quad (5)$$

Further uncertainty comes in relating the Fe core mass to the compact core mass. It can, however, be seen from Table 3 of Brown, Weingartner, & Wijers (1996) that the estimated fallback mass following separation in the supernova explosion roughly compensates for the binding energy increase in going from

the Fe core to the compact object. Thus, we will assume the compact object masses to be the same as those of the Fe cores. In addition to the uncertainty in this relation, there is the further uncertainty that the fallback mass, which is dependent on the density structure in the layers above the Fe core (Fryer 1999; Janka 2001), is unknown, since consistent supernova explosions have not been achieved.

None the less, we believe it useful to move ahead with our estimated M_{PC} which indicates that single stars with ZAMS masses $\gtrsim 20 M_{\odot}$ go into high-mass black holes. Brown, Lee, & Tauris (2001) recently showed that given presently accepted wind losses (Schaller et al. 1992) the high mass black holes in the transient sources with main sequence companion can only be evolved in the region of ZAMS mass $\sim 20 M_{\odot}$, so our choice of M_{PC} is supported to this extent by evolutionary arguments.

We note briefly that SN 1987A, if it formed a black hole, went into a low mass black hole of mass $1.5 M_{\odot} < M_{BH} < 1.8 M_{\odot}$ according to the Brown & Bethe (1994) estimates. The black hole would have a low mass in this interval because the He envelope was blown off in the delayed explosion. Note from Fig. 2 of main sequence masses that there is only a narrow interval from $\sim 18 M_{\odot}$ to $20 M_{\odot}$ in which this could happen given the above interval.

Schaller et al. (1992) use a $^{12}\text{C}(\alpha, \gamma)^{16}\text{O}$ S-factor of $S(300 \text{ keV}) \sim 100 \text{ keV barns}$ as compared with the Woosley & Weaver 170 keV barns. They bring their central abundance down to 0.16 at the end of core He burning only for a ZAMS $25 M_{\odot}$ star, so presumably this would be the mass at which the Fe cores would begin to rise rapidly in mass with further evolution. We believe the Weaver & Woosley value for the $^{12}\text{C}(\alpha, \gamma)^{16}\text{O}$ rate to be more correct (Boyes, Heger, & Woosley 2001), placing the narrow interval of ZAMS masses from which SN 1987A can be evolved correctly. In fact, most recently experiments including both E1 and E2 components have been carried out (Kunz et al. 2001), obtaining $S_{tot}^{300} = (165 \pm 50) \text{ keV barns}$.

4 Possible Evolution of Cyg X-1

4.1 Space Velocity vs the Mass Loss in the Formation of Cyg X-1

According to the calculations of Wellstein & Langer (1999) and Fryer et al. (2001), it is unlikely that a black hole as massive as the $10 M_{\odot}$ core (Herrero et al. 1995) in Cyg X-1 can be evolved from a naked He star (see Table 1 and Fig. 2). Although the calculations of naked He stars were extended up to only ZAMS $60 M_{\odot}$ stars, the He winds scale with the 2.6 power of the mass, so

that higher mass He stars would be expected to behave in the same way. In fact, Wellstein & Langer (1999) and Fryer et al. (2001) were unable to evolve a $10 M_{\odot}$ black hole, whereas the high space velocity of Cyg X-1, $49 \pm 14 \text{ km s}^{-1}$ (Kaper et al. 1999) indicates substantial mass loss in a Blaauw-Boersma kick (Blaauw 1961; Boersma 1961) in the black hole formation, increasing the necessary He core mass. We now estimate this mass loss, following the development of Nelemans et al. (1999). It is reasonable to evolve Cyg X-1 analogously to the soft X-ray black hole transient sources, the difference being in the high mass companion star which presumably makes Cyg X-1 shine continuously.

The high space velocity of Cyg X-1 can be explained by mass loss in the black hole formation, because this loss from the black hole is somewhat off from the center of gravity of the system. From Nelemans et al. (1999), the runaway velocities from symmetric SNe (See Appendix for the derivation)

$$v_{sys} = 213 \times \Delta M \times m \times P_{re-circ}^{-1/3} \times (M_{BH} + m)^{-5/3} \text{ km s}^{-1} \quad (6)$$

where masses are in M_{\odot} , P in days, and $\Delta M = M_{He} - M_{BH}$ with M_{He} the He star mass of the Black hole progenitor. Here $P_{re-circ}$ is the re-circularized orbital period after Blaauw-Boersma kick, and we assume no orbital evolution ($P_{re-circ} = P_{obs}$) since the beginning of the mass transfer phase, and neglect small eccentricity as in Nelemans et al. (1999). By putting in average values,

$$v_{sys} = 8.32 \times \Delta M \text{ km s}^{-1}. \quad (7)$$

In order to obtain the observed velocity, we need $\Delta M \sim 5.9 M_{\odot}$, indicating the black hole progenitor mass to be $M_{He} \sim 16 M_{\odot}$. Note that this ΔM and M_{He} are in the same ballpark as those estimated by Nelemans et al. for Nova Scorpii 1994(GRO J1655–40). This suggests that the evolution of Cyg X-1 is similar to that of Nova Scorpii 1994, except that the progenitor mass of the black hole must be much higher in Cyg X-1 and the companion is an O-star rather than an F-star.

The current orbital separation of Cyg X-1 is

$$a_{\text{now}} \approx 4.2 R_{\odot} \left(\frac{P_{orb}}{\text{days}} \right)^{2/3} \left(\frac{M_{BH} + M_O}{M_{\odot}} \right)^{1/3} \approx 40 R_{\odot}. \quad (8)$$

Before the explosion, the orbital separation of the black hole progenitor and companion star was

$$a_{\text{preSN}} \approx \frac{a_{\text{now}}}{1 + e_2} \approx 33 R_{\odot} \quad (9)$$

where $e_2 = \Delta M/(M_{\text{BH}} + M_O) \approx 0.21$ is the eccentricity right after the supernova explosion. For the derivation, see Appendix. This is only slightly larger than the $30 R_\odot$ estimated by Bethe & Brown (1999) for the minimum initial separation of the O-star progenitors. If the progenitors were initially closer together they would merge already at this stage of evolution.

As noted by Bethe & Brown (1999), the two O-star progenitors must have initially had a separation of nearly $33 R_\odot$. Substantial mass loss, especially by the WR star would have been expected to widen the orbit substantially

$$\frac{a_f}{a_i} = \frac{M_i}{M_f} \sim 2 - 3 \quad (10)$$

where M_i and M_f are the initial and final system masses. In order to tighten the orbit to the $33 R_\odot$ we find before the massive star goes into a black hole, there must have been some period of nonconservative mass transfer.

4.2 Extended WNL Stage of Black Hole Progenitor

Langer (1989b) finds that towards the end of core hydrogen burning the radius of a massive star may be much larger than its radius on the zero age main sequence. For example, a $100 M_\odot$ star increases its radius from $13 R_\odot$ at H ignition by a factor ~ 4 to $53 R_\odot$ at core H exhaustion. In the evolutionary phase between central H- and He-burning massive stars develop an intermediate fully convective zone just above the H-burning shell which reaches its maximal spatial extent and $\sim 18 M_\odot$ in mass for the $100 M_\odot$ star (Langer 1987). There may be further expansion in a hydrogen shell burning stage unless large mass loss sets in. But the latter may begin only later in the LBV stage. In any case, there will be a period before or in the LBV stage where the hydrogen is being propelled outwards, but does not yet have enough velocity to escape. A companion to the very massive star will, if in this region, couple hydrodynamically to the hydrogen in the manner explicitly worked out by Bethe & Brown (1999), and furnish energy to it from a drop in its gravitational binding; i.e., through some mechanism resembling common envelope evolution. We cannot be more explicit, because of the uncertainty in the post main sequence evolution of the very massive stars, but some nonconservative mass transfer seems to be necessary in the evolution of a binary such as Cyg X-1. We admit to being in somewhat of a predicament, however, since we do not want a common envelope evolution which removes the hydrogen before the helium burning is well underway.

It is clear that the black hole in Cyg X-1 cannot have evolved from a naked He star. An important clue to its possible evolution is offered by the evolution of

WLW (1993) of a ZAMS $85 M_{\odot}$ star, where the WR stage began with a WNL stage which took $\sim 40\%$ of the total WR time. (Their $60 M_{\odot}$ star also had a WNL stage, but it took only $\sim 25\%$ of the WR time.) During this time the WR is covered by hydrogen and the attendant mass loss rate is much lower than that for a naked He star.

Using the times for each WR stage as WLW 1995, we calculate in Table 3 the masses for ZAMS $60 M_{\odot}$ and $85 M_{\odot}$ stars. Of course there is feedback on these masses from the change in times of each stage with altered mass loss rate. In order to take the feedback into account, we use the ratios of M_{CO} cores calculated by Fryer et al. (2001) for a ZAMS $60 M_{\odot}$ star for various mass loss rates to the original WLW (1995) one as plotted in Fig 3.

We note from Table 3 that a ZAMS $60 M_{\odot}$ star with WR stage mass loss rate reduced by $1/3$ loses $1.7 M_{\odot}$ during its WNL stage, at an average rate of $1.5 \times 10^{-5} M_{\odot} \text{ yr}^{-1}$. This is an order of magnitude less than it would lose as a WNE (bare) He star, and explain why the final He star mass can be as large as $13.5 M_{\odot}$. The WNL mass loss rate is ~ 2.25 times the main sequence mass rate for a ZAMS $60 M_{\odot}$ star of Castor, Abbott, & Klein (1975).

In Fig. 3 we plot our ratios from Table 3 for He star masses alongside the Fryer et al. (2001) ratios of CO core masses. The divergence in our favored range of $1/2 - 1/3$ is not large, so we believe our procedure in calculating masses is justified. We see from Table 3 that we need a mass loss rate of ~ 0.4 times the WLW (1995) one in order to lose $\sim 6 M_{\odot}$ in the explosion and to be left with an $\sim 10 M_{\odot}$ black hole.

4.3 Discussion on Cyg X-1 Type Objects

We want to point out that there is a strong metallicity dependance in our model. As the winds of WNL stars are likely radiation driven (Hamann et al. 2000), we can expect them to weaken with smaller metallicity. Thus, the lower limit of the initial mass range from which the the final stellar mass can grow again will be decreasing. Therefore, we expect more Cyg X-1 type systems at lower metallicity. We also would like to point out that there is dependance in mixing processes, in particular rotation, which can increase the lower limit of the initial mass range.

Using standard population synthesis, Bethe & Brown (1999) estimated that there should be ~ 7 Cyg X-1 like objects in the Galaxy, where we see only one (leaving out LMC X-1 and LMC X-3). Although the γ -rays from such an object easily penetrate the Galactic disc, they would not be distinguished from those from gamma ray bursts (Maarten Schmidt, private communication 2001).

As possible WR progenitor of the Cyg X-1 black hole, we suggest “WR22”; the most massive Wolf-Rayet ever weighed (Rauw et al. 1996). The minimum Wolf-Rayet mass is $72 M_{\odot}$ and the mass ratio to O-star is 2.78, giving an O-star mass of $> 26 M_{\odot}$. The spectrum of the WN7 exhibits a considerable amount of hydrogen ($X_H \sim 40\%$, Hamann et al. 1991, Crowther et al. 1995), strong WR emission lines and absorption lines that belong to the WR component (Niemela 1973; Moffat & Seggewiss 1978). Rauw et al. (1996) identify the companion as an O-star. With ~ 80 day period, the binary is, however, much too wide in order to narrow sufficiently in common envelope evolution to produce a Cyg X-1 type binary, according to the Bethe & Brown (1999) estimates.

5 Conclusion

Our conclusion to all of the above is simple: In order to evolve high-mass black holes at solar metallicity, the He core of the massive star must be covered by hydrogen at least most of the time, while it burns.

For SXTs, the stars in the mass range $\sim 20 - 35 M_{\odot}$ could evolve into high-mass black holes with the condition that their H envelope was lifted off by the companion star only after the He core burning was complete. For more massive stars like Cyg X-1 type objects, an extended WNL stage could drive the formation of high-mass black holes.

Acknowledgments

We thank Stan Woosley for many helpful discussions and are indebted to Tom Weaver for supplying us with his grid of stellar evolution models. We wish to thank Maarten Schmidt for communication about the indistinguishability of further Cyg X-1 like objects from gamma ray bursts. This work was partially supported by the U.S. Department of Energy under Grant No. DE-FG02-88ER40388, by the Alexander von Humboldt-Stiftung through Grant FLF-1065004, by 2000-2001 KIAS Research Fund, and by the Deutsche Forschungsgemeinschaft through Grants La 587/15 and La 587/16.

Appendix. Blaauw-Boersma Kick

In this Appendix, the details of the Blaauw-Boersma kick (Blaauw 1961, Boersma 1961) are summarized. Before the explosion,¹ from Fig. 4 (a), R_{He} , v_{He} , and ω_1 are given as

$$\begin{aligned} R_{He} &= \left(\frac{m}{M_{He} + m} \right) a_1 \\ v_{He} &= \frac{1}{a_1} (GmR_{He})^{1/2} \\ \omega_1 &= \left(\frac{m}{M_{He} + m} \right) \left(\frac{Gm}{R_{He}^3} \right)^{1/2}. \end{aligned} \quad (\text{A.1})$$

After the explosion, we assume that $\Delta M \equiv M_{He} - M_{BH}$ was lost from the BH progenitor without interacting with the binary system. The momentum lost from the binary system should be compensated by the space velocity of the new binary system.

$$\Delta p = \Delta M \cdot v_{He} = (M_{BH} + m) \cdot v_{sys} \quad (\text{A.2})$$

which gives the space velocity of the new binary system (c.m. motion of B)

$$v_{sys} = \left(\frac{\Delta M}{M_{BH} + m} \right) v_{He}. \quad (\text{A.3})$$

Right after the explosion, in the new c.m. frame of BH and O-star binary, by defining the semi-major axis d_2 and the eccentricity e_2 , we have

$$\begin{aligned} \omega_2 &= \left(\frac{m}{M_{BH} + m} \right) \left(\frac{Gm}{d_2^3} \right)^{1/2} \\ R_{BH} &= \left(\frac{m}{M_{BH} + m} \right) a_1 \\ v_{BH} &= v_{He} + v_{sys} = \left(\frac{M_{He} + m}{M_{BH} + m} \right) v_{He}. \end{aligned} \quad (\text{A.4})$$

Since the v_{BH} is greater than that of the circular motion with radius R_{BH}

¹ Subscript 1 (2) indicates the properties before (right after) the explosion, and subscript “now” indicates the current properties observed.

$$\begin{aligned} v_{BH} &= \left(\frac{M_{He} + m}{M_{BH} + m} \right)^{1/2} v_{circ} > v_{circ} \\ v_{circ} &= \left(\frac{Gm^2}{a_1(M_{BH} + m)} \right)^{1/2}, \end{aligned} \quad (\text{A.5})$$

one can conclude that R_{BH} is at the minimum of the orbital separation, i.e.

$$R_{BH} = d_2(1 - e_2). \quad (\text{A.6})$$

Note that \vec{v}_{BH} and \vec{R}_{BH} are perpendicular right after the explosion as in Fig. 4 (c).

The orbital angular momentum of the BH can be expressed using a_2 and e_2

$$l_a = [Gm\mu^2 d_2(1 - e_2^2)]^{1/2} = [Gm\mu^2 R_{BH}(1 + e_2)]^{1/2} \quad (\text{A.7})$$

or

$$l_b = M_{BH} R_{BH} v_{BH} = \mu a_1 v_{BH} = \mu (GmR_{BH})^{1/2} \left(\frac{M_{He} + m}{M_{BH} + m} \right)^{1/2} \quad (\text{A.8})$$

where μ is the reduced mass

$$\mu = \frac{M_{BH} m}{M_{BH} + m}. \quad (\text{A.9})$$

By equating $l_a = l_b$ we have

$$e_2 = \frac{\Delta M}{M_{BH} + m}. \quad (\text{A.10})$$

We assume that there is no angular momentum lost during the circularization process by tidal locking after SN explosion. From angular momentum conservation

$$l_{now} = (Gm\mu^2 d_{now})^{1/2} = [Gm\mu^2 d_2(1 - e_2^2)]^{1/2}. \quad (\text{A.11})$$

Therefore, from

$$d_{now} = \left(\frac{m}{M_{BH} + m} \right) a_{now}$$

$$= d_2(1 - e_2^2) = R_{BH}(1 + e_2) = \left(\frac{m}{M_{BH} + m} \right) a_1(1 + e_2) , \quad (\text{A.12})$$

we have the relation of the orbital separations

$$a_{now} = a_1(1 + e_2) . \quad (\text{A.13})$$

Using this relation, one have

$$\begin{aligned} \omega_1 &= (1 + e_2)^2 \omega_{now} \\ \omega_2 &= (1 - e_2^2)^{3/2} \omega_{now} \end{aligned} \quad (\text{A.14})$$

or the period relations

$$P_{now} = (1 - e_2^2)^{3/2} P_2 = (1 + e_2)^2 P_1 . \quad (\text{A.15})$$

Now Eq. (A.3) can be expressed in terms of observed quantities using

$$\begin{aligned} a_{now} &= \left(\frac{P_{now}}{2\pi} \right)^{2/3} \left[G(M_{BH} + m) \right]^{1/3} \\ v_{He} &= \left(\frac{1 + e_2}{a_{now}} \right)^{1/2} \left(\frac{Gm^2}{M_{He} + m} \right)^{1/2} = \left[\frac{1}{a_{now}} \left(\frac{Gm^2}{M_{BH} + m} \right) \right]^{1/2} \\ &= \frac{(2\pi G)^{1/3} m}{(M_{BH} + m)^{2/3} P_{now}^{1/3}} . \end{aligned} \quad (\text{A.16})$$

Finally the Blaauw-Boersma kick velocity becomes

$$\begin{aligned} v_{sys} &= \frac{\Delta M}{M_{BH} + m} v_{He} = \frac{(2\pi G)^{1/3} \Delta M m}{(M_{BH} + m)^{5/3} P_{now}^{1/3}} \\ &= 213 \left(\frac{\Delta M}{M_\odot} \right) \left(\frac{m}{M_\odot} \right) \left(\frac{P_{now}}{\text{days}} \right)^{-1/3} \left(\frac{M_{BH} + m}{M_\odot} \right)^{-5/3} \text{ km s}^{-1} . \end{aligned} \quad (\text{A.17})$$

References

Abbott, D.C., Bieging, J.H., Churchwell, E., and Torres, A.V. 1986, ApJ 303, 239
 Bethe, H. A. and Brown, G. E. 1999, ApJ, 517, 318
 Bethe, H. A., Brown, G. E., Applegate, J.H., and Lattimer, J. 1979, Nuclear Physics A, 324, 487

Blaauw, A. 1961, *Bull. Astron. Inst. Netherlands*, 15, 265

Boersma, J. 1961, *Bull. Astron. Inst. Netherlands*, 15, 291

Boyes, M.M., Heger, A., and Woosley, S.E. 2001, in preparation

Brown, G.E. and Bethe, H.A. 1994, *ApJ*, 423, 659

Brown, G.E., Lee, C.-H., and Bethe, H.A. 1999, *New Astronomy*, 4, 313

Brown, G.E., Lee, C.-H., and Tauris, T. 2001, *New Astronomy*, submitted; astro-ph/0102001

Brown, G.E., Weingartner, J.C., and Wijers, R.A.M.J. 1996, *ApJ*, 463, 297

Chiosi, C. and Maeder, A. 1986, *ARA&A*, 24, 329

Castor, J.I., Abbott, D.C., and Klein, R.I. 1975, *ApJ*, 195, 157

Crowther, P.A., Hillier, D.J., and Smith, L.J. 1995, *A&A*, 293, 403

Fryer, C.L. 1999, *ApJ*, 522, 413

Fryer, C.L., Heger, A., Wellstein, S. and Langer, N. 2001, in preparation

Fuller, G. M., Fowler, W. A. and Newman, M. J. 1985, *ApJ*, 293, 1

Hamann W.-R., Koesterke, L., 1998, *A&A* 335, 1003

Hamman, W.-R., Dünnebeil, G., Koesterke, L., Schmutz, W., and Wessolowski, U. 1991, *A&A*, 249, 443

Hamann, W.-R., Koesterke, L., and Gräfener, G., 2000, in: *ASP Conf. Ser.* 204, *Thermal and Ionization Aspects of Flows from Hot Stars*, H. Lamers, A. Sapar, eds., p. 197

Heger, A., Langer, N., and Woosley, S.E. 2000, *ApJ*, 528, 368

Heger, A., Woosley, S.E., Martinez-Pinedo, G., and Langanke, K.-H. 2001, astro-ph/0011507

Herrero, A., Kudritzki, R.P., Gabler, R., Vilchez, J.M., and Gabler, A. 1995, *A&A*, 297, 556

Janka, H.-Th. 2001, *A&A*, 368, 527

Kaper, L., Camerón, A., and Barziv, O. 1999, in *Wolf-Rayet phenomena in massive stars and starburst galaxies*, IAU Symp. 193, eds. K.A. van der Hucht, G. Koenigsberger, and R.J. Eenens, p. 316

Khaliullin, K.F., Khaliullina, A.I., and Cherepashchuk, A.M. 1984, *Sov. Astron. Lett.*, 10, 250

Kunz, R., Jaeger, M., Mayer, A., Hammer, J.W., Starudt, G., Harissopolus, S., and Paradellis, T. 2001, *Phys. Rev. Lett.*, 86, 3294.

Langanke, K., and Martinez-Pinedo, Nucl., G. 2000, Phys. A, 673, 481

Langer, N. 1987, A&A 171, L1

Langer, N. 1989a, A&A 220, 135

Langer, N. 1989b, Rev. Mod. Astron., 2, 306

Langer, N. and El Eid, M.F. 1986, A&A 167, 265

Marchenko, S.V., Moffat, A.F.J., and Koenigsberger, G. 1994, ApJ, 422, 810

Moffat, A.F.J. and Robert, C. 1994, ApJ, 421, 310

Moffat, A.F.J. and Seggewiss, W. 1978, A&A, 70, 69

Nelemans, G., Tauris, T. M., and van den Heuvel, E. P. J. 1999, A&A, 352, L87

Niemela, V.S. 1973, PASP, 85, 220

Nugis, T. and Lamers, H.J.G.L.M. 2000, A&A, 360, 227

Rauw, G., Vreux, J.-M., Gosset, E., Hutsemékers, D., Magain, P., and Rochowicz, K. 1996, A&A, 306, 771

Schaller, G., Schaerer, D., Meynet, G., and Maeder, A. 1992, A&AS, 96, 269

St.-Louis, N., Moffat, A.F.J., Lapointe, L., Efimov, Y.S., Shakhovskoy, N.M., Fox, G.K., and Piirola, V. 1993, ApJ, 410, 342

Stothers R.B., 2000, ApJ 530, L103

Thorsett, S.E. and Chakrabarty, D. 1999, ApJ, 512, 288

Timmes, F.X., Woosley, S.E., and Weaver, T.A. 1996, ApJ, 457, 834

Weaver, T.A., Zimmerman, G.B., and Woosley, S.E. 1978, ApJ, 225, 1021

Weaver, T.A. and Woosley, S.E. 1993, Physics Reports, 227, 65

Wellstein, S. and Langer, N. 1999, A&A, 350, 148

Woosley, S.E., Langer, N., and Weaver, T.A. 1993, ApJ, 411, 823

Woosley, S.E., Langer, N., and Weaver, T.A. 1995, ApJ, 448, 315

Woosley, S.E. and Weaver, T.A. 1995, ApJS, 101, 181

| Model | M_{MS} | M_{comp} | C_c | M_{He} | M_{CO} | M_{Fe} | Mass Transfer |
|-------|----------|------------|-------|----------|----------|----------|---------------|
| 1s | 60 | 34 | 0.30 | | 3.37 | 1.35 | B |
| 2s | 60 | 34 | 0.32 | 4.07 | 3.07 | 1.50 | A+AB |
| 5s | 40 | 30 | 0.33 | 3.84 | 2.87 | 1.49 | A+AB |
| 7s | 30 | 24 | 0.34 | 3.63 | 2.71 | 1.46 | A+AB |
| 10s | 25 | 24 | 0.36 | 3.39 | 2.42 | 1.49 | A+AB |
| 17s | 20 | 18 | 0.36 | 3.39 | 2.18 | 1.56 | B |

C_c : Central Carbon abundance

Masses : in unit of M_\odot

Table 1

Results of Wellstein & Langer (1999) and Fryer et al. (2001) with reduced WR mass loss rate, 1/2 of WLW (1993) value, at the end of central He burning. The M_{Fe} is the final Fe core mass.

| Model | Mass Loss Rate* | C_c | τ_C | $M_{CO}[M_\odot]$ | $M_{Fe}[M_\odot]$ |
|-------|-----------------|-------|----------|-------------------|-------------------|
| 1s1 | 1 | 0.35 | 3800 yrs | 2.35 | 1.32 |
| 1s2 | 1/2 | 0.30 | 1600 yrs | 3.37 | 1.35 |
| 1s3 | 1/3 | 0.27 | 700 yrs | 4.76 | 1.61 |
| 1s4 | 1/4 | 0.25 | 500 yrs | 5.93 | 1.75 |
| 1s6 | 1/6 | 0.22 | No | 8.53 | 1.50 |

* Ratio of WR mass loss to that of WLW 1993

C_c : Central Carbon abundance

τ_C : Convective carbon core burning time

Table 2

Results of Wellstein & Langer (1999) and Fryer et al. (2001) for different mass loss rates of a ZAMS $60 M_\odot$ star at the end of central He burning. Models “1s#” correspond to the binary system (ZAMS $60 M_\odot$ and $34 M_\odot$) with Case B mass transfer.

| $60 M_{\odot}$ WRB | WR Stage Mass Loss Rate | | | | | | $\tau (10^5 \text{ yrs})$ |
|--------------------|-------------------------|------|------|------|------|------|---------------------------|
| | 1 | 1/2 | 0.4 | 1/3 | 1/4 | 1/6 | |
| pre WR stage | 26.5 | 26.5 | 26.5 | 26.5 | 26.5 | 26.5 | 1.13 (25%) |
| post WNL | 22.5 | 24.2 | 24.5 | 24.8 | 25.1 | 25.6 | |
| post WNE | 11.5 | 15.4 | 16.5 | 17.5 | 18.9 | 20.8 | |
| post WC/WO | 6.65 | 9.60 | 10.7 | 11.6 | 13.2 | 15.5 | |
| after feedback* | 6.65 | 9.53 | 11.9 | 13.5 | 16.8 | 24.1 | |

| $85 M_{\odot}$ WRB | WR Stage Mass Loss Rate | | | | | | $\tau (10^5 \text{ yrs})$ |
|--------------------|-------------------------|------|------|------|------|------|---------------------------|
| | 1 | 1/2 | 0.4 | 1/3 | 1/4 | 1/6 | |
| pre WR stage | 45.3 | 45.3 | 45.3 | 45.3 | 45.3 | 45.3 | 1.40 (41%) |
| post WNL | 34.3 | 40.0 | 40.8 | 41.6 | 42.5 | 43.4 | |
| post WNE | 14.7 | 20.9 | 23.0 | 24.7 | 27.5 | 31.2 | |
| post WC/WO | 9.7 | 14.3 | 16.1 | 17.6 | 20.2 | 24.0 | |
| after feedback* | 9.7 | 13.9 | 17.3 | 19.6 | 24.5 | 35.2 | |

* scaled by the numerical results of Fryer et al. (Fig. 3)

Table 3

Mass-loss-rate-dependences of masses (in M_{\odot}) at the different stages of WR stars (models 60WRB and 85WRB of WLW93). The WR stage mass loss rates are in units of standard rate of WLW93. The same WR stage times of WLW93 are used for different mass loss rates.

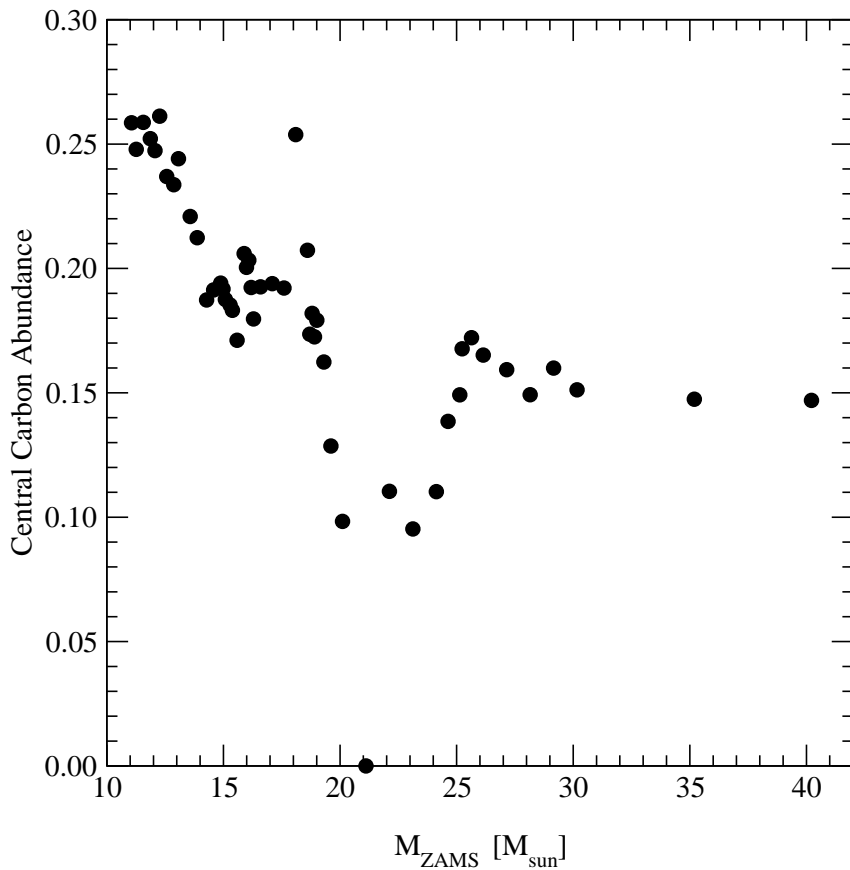


Fig. 1. Central carbon abundance at the end of He core burning for “clothed” (single) stars as function of ZAMS mass. The calculation was carried out by Tom Weaver (1995, priv. com.) using the KEPLER code (Weaver, Zimmerman, & Woosley 1978; Woosley & Weaver 1995). The rapid drop in C_c at ZAMS mass $M_{ZAMS} \sim 20 M_\odot$ signals the disappearance of convective carbon burning.

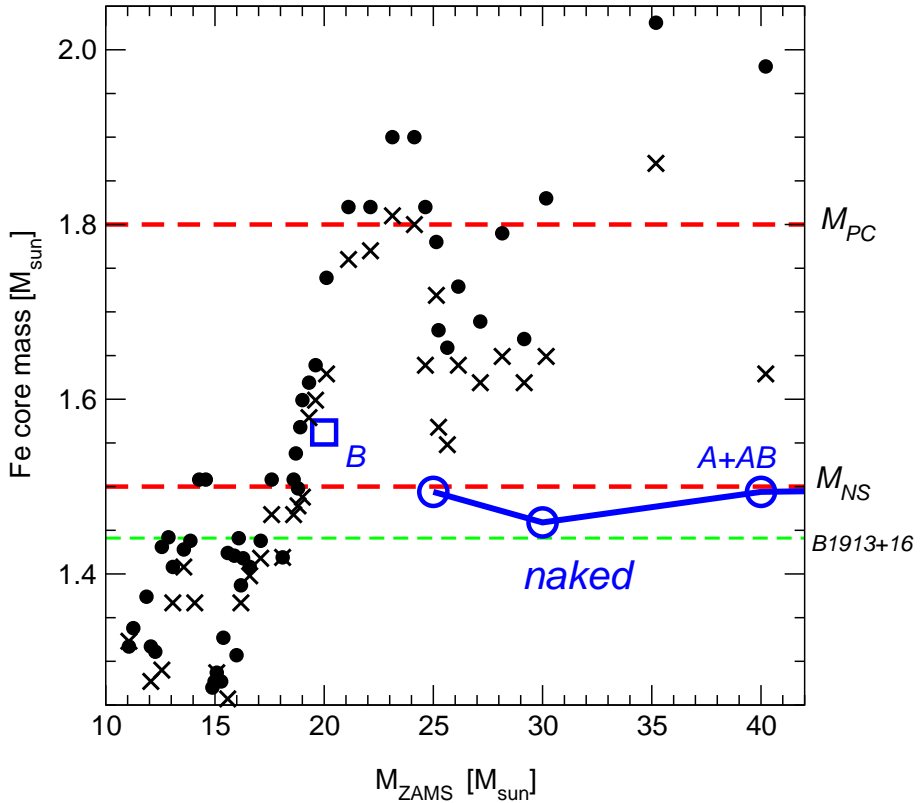


Fig. 2. Comparison of the iron core masses resulting from the evolution of “clothed” and “naked” He cores. Filled circles and crosses correspond to the core masses of “clothed” stars at the time of iron core implosion for a finely spaced grid of stellar masses (Heger, Woosley, Martinez-Pinedo, & Langanke 2001). The circular were calculated with the Woosley & Weaver 1995 code, whereas the crosses employ the vastly improved Langanke, Martinez-Pinedo (2000) rates for electron capture and beta decay. Open circles (square) correspond to the naked He stars in case A+AB (B) mass transfer of Fryer et al. (2001), with reduced WR mass loss rate, see Table 1. If the assembled core mass is greater than $M_{PC} = 1.8 M_{\odot}$, where M_{PC} is the proto-compact star mass as defined by Brown & Bethe (1994), there is no stability and no bounce; the core collapses into a high mass black hole. $M_{NS} = 1.5 M_{\odot}$ denotes the maximum mass of neutron star (Brown & Bethe 1994). The mass of the heaviest known well-measured pulsar, PSR B1913+16, is also indicated with dashed horizontal line (Thorsett & Chakrabarty 1999).

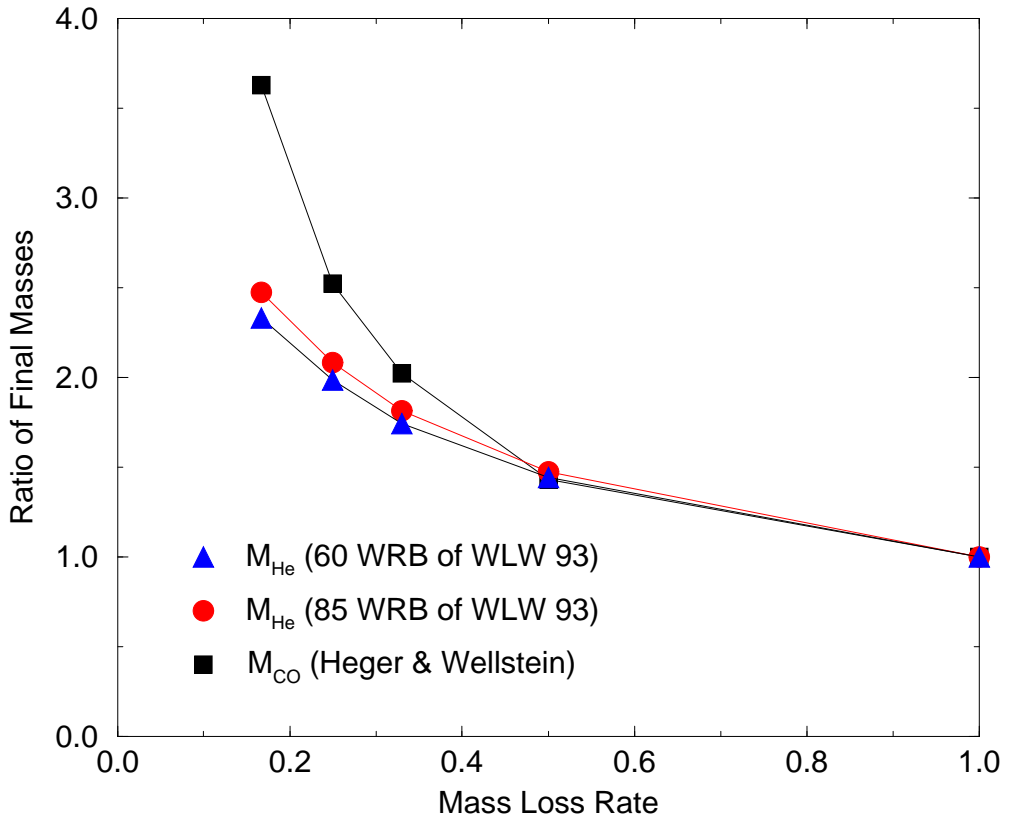


Fig. 3. Mass-loss-rate-dependences of final CO core masses M_{CO} (filled square) from the $60 M_{\odot}$ star discussed in Fryer et al. (2001) and final He core masses (filled triangles and circles for $60 M_{\odot}$ and $85 M_{\odot}$, respectively) after WR stage from Tab. 1. The masses are scaled by those with standard rate of WLW93.

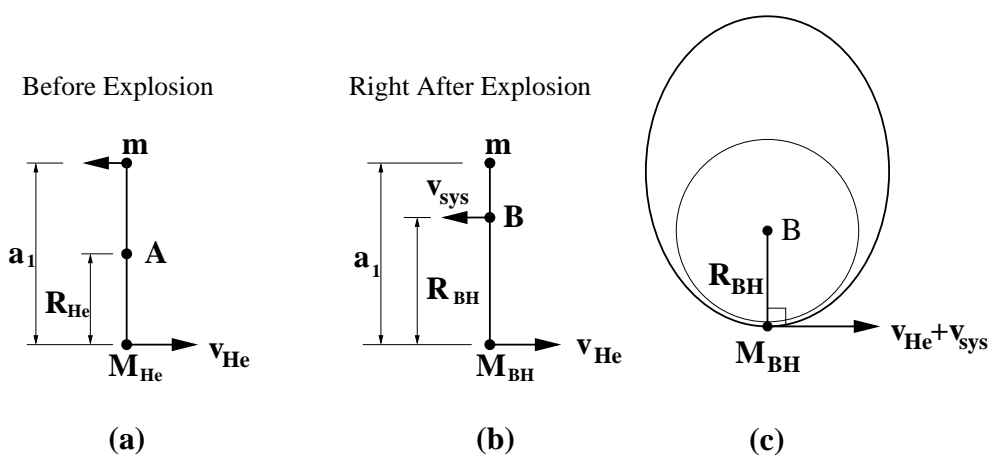


Fig. 4. Coordinates (a) before the explosion in the c.m. frame, (b) right after the explosion in the original c.m. frame, and (c) in the new c.m. frame of black hole and companion right after the explosion.